ELSEVIER

Available online at www.sciencedirect.com

ScienceDirect

Control Engineering Practice 00 (2016) 1–14

Control Eng. Pract.

Optimal Pressure Sensor Placement and Assessment for Leak Location[1] Using a Relaxed Isolation Index: Application to the Barcelona Water Network☆

Miquel À. Cugueró-Escofet, Vicenç Puig, Joseba Quevedo[a]

[a]*Supervision, Safety and Automatic Control Research Center (CS2AC), Polytechnic University of Catalonia (UPC), Terrassa Campus, Gaia Research Bldg., Rambla Sant Nebridi, 22. 08222 Terrassa, Barcelona, Spain (e-mail: {miquel.angel.cuguero,vicenc.puig,joseba.quevedo}@upc.edu).*

Abstract

Water distribution networks are large complex systems that are affected by leaks, which often entail high costs and may severely jeopardise the overall water distribution performance. Successful leak location[1] is paramount in order to minimize the impact of these leaks when occurring. Sensor placement is a key issue in the leak location[2] process, since the overall performance and success of this process highly depends on the choice of the sensors gathering data from the network. Common problems when isolating leaks in large scale highly-gridded real water distribution networks include leak mislabelling and large location areas obtention due to similarity of leak effect in the measurements, which may be caused by topological issues and led to incomplete coverage of the whole network. The sensor placement strategy may minimize these undesired effects by setting the sensor placement optimisation problem with the appropriate assumptions (e.g. geographically cluster alike leak behaviors) and taking into account real aspects of the practical application such as the acceptable leak location distance. In this paper, a sensor placement methodology considering these aspects and a general sensor distribution assessment method for leak diagnosis in water distribution systems is presented and exemplified with a small illustrative case study. Finally, the proposed method is applied to two real District Metered Areas (DMAs) located within the Barcelona water distribution network.

Keywords: Sensor placement, fault detection and isolation, leak location[3], correlation coefficient, water distribution networks.

1. Introduction

An issue of great concern in water drinking networks is the existence of leaks at the distribution stage, highly related with water resource savings and management costs. The traditional approach to leak control is a passive one, whereby the leak is repaired when it becomes visible. Recently developed acoustic instruments also allow non-visible leak location [1], but their application in large-scale water networks is very expensive and time-consuming. A viable

[1]R4-C4
[1]R4-C4
[2]R4-C4
[3]R4-C4

☆This work has been partially funded by the Spanish Ministry of Science and Technology through the Project ECOCIS (Ref. DPI2013-48243-C2-1-R) and Project HARCRICS (Ref. DPI2014-58104-R), and by EFFINET grant FP7-ICT-2012-318556 of the European Commission.

solution to this problem is to divide the network into District Metered Areas (DMAs), where the *flow* and the *pressure* are measured [2, 3], and to maintain a permanent leak control-system. Leaks in fact increase the flow and decrease the pressure measurements at the DMA inputs. Several empirical studies propose mathematical models to describe the leak flow with respect to the pressure at the leak location [4, 5]. Best practice in the analysis of DMA flows consists in the estimation of the leak when the flow is minimum. This typically occurs at night time, when customers' demand is low and the leak component is at its highest percentage over the flow [3]. Therefore, an accepted approach by the practitioners[2] is to monitor the DMA or groups of DMAs in order to detect and repair the leaks occurring by analyzing the minimum night flow, and also to employ techniques to estimate the corresponding leak magnitude [3]. However, leak detection may not be easy to perform, since unpredictable variations in the customers' demand and measurements noise may occur, as well as long-term trends and seasonal effects.[3]

Several works in the literature have addressed the leak location problem in DMAs. In [6], a review of transient-based leak detection methods is summarized. In the seminal work [7], a model-based leak detection and location[4] is solved by means of a least-squares estimation problem. The latter problem is, however, not easy to solve when considering the non-linear models involved. Alternatively, a method based on pressure measurements and leak sensitivity analysis is proposed in [8], where a set of residuals (generated as the difference between pressure measurements provided by several sensors installed within the DMA and their estimations by the network hydraulic model) is analysed considering a certain threshold which takes into account practical factors e.g. the model uncertainty and the measurement noise. This approach shows satisfactory results under ideal conditions, but its performance degrades when considering nodal demand uncertainty and measurement noise. This technique is improved in [9], where an extended time horizon analysis is considered and a comparison of the performance using different metrics is performed.

The performance of the leak location[5] approach is highly dependent on the sensor number and placement within the DMA. Hence, the sensor placement strategy is a key issue to consider in the overall process. There is an important trade-off between the number of sensors and the subsequent cost which prevents the use of a high number of sensors for leak location purposes. Consequently, this number should be optimised at the sensor placement stage in order to produce the highest possible benefit, that is, maximize the leak location performance at the minimum cost. According to these constraints, the sensors considered here are pressure sensors since they are a cheaper alternative to flow meters for the company managing the network, but the methodology presented might also be applied using different sensor setups if required e.g. combining pressure and flow meters as in [10] or chlorine meters for water quality fault diagnosis. Hence, the methodology may be arranged with minor modifications to different fault diagnosis purposes and schemes.[6]

Regarding sensor placement for fault detection and isolation (FDI) purposes, several works may be found in the literature concerning this subject. Some approaches consider the study of structural matrices in order to locate sensors based on isolability criteria [11]. In [12], an optimal set of sensors for model-based FDI is sought by means of an optimisation method based on binary linear programming. These works are embraced in the general framework of FDI of dynamic systems. However, they are not specially suited to consider the non-explicit non-linear set of equations describing a water distribution network. Alternatively, several works treated the sensor placement problem when applied to water distribution networks, most of them addressing the water contamination monitoring (e.g. [13, 14]), where sensor placement is considered in a large water distribution network in order to detect malicious introduction of contaminants. Regarding leak location[7], less contributions addressed the problem of sensor placement. This problem is studied in [15], where an strategy based on the leak isolability maximization is considered to optimally place the sensors based on the water network structural model, and in [8], where an optimal sensor placement is formulated as an integer programming problem, similarly as presented here. Also, an entropy-based approach for efficient water loss incident detection is introduced in [16].

Furthermore, leak location[8] in real water networks involves discrimination among a high number of possible leak locations (typically, the DMA nodes) leading to mislabel the right one due to the limited number of sensors available.

[2] R4-C6
[3] R2-C3
[4] R4-C4
[5] R4-C4
[6] R4-C7
[7] R4-C4
[8] R4-C4

However, in practice it is not needed to locate the leak at the exact place since final on-the-ground leak location[9] techniques (e.g. ground-penetrating radar, acoustic listening devices [17]) may locate leaks in a precise way starting from an area close to where the actual leak is occurring. Hence, this calls for a methodology of sensor placement trying to cluster similar leak behaviors geographically in order to minimize the number of installed sensors and locate the leak within a certain cluster distance precision.

Having all this into account, here a new approach for sensor placement focused on leak location[10] in DMAs is proposed, based on the method introduced in [18]. Alternatively to [8], the approach presented here does not binarize the sensitivity matrix, hence the complete numerical precision of this matrix is used, leading to better leak location[11] performance as pointed out in [18, 9]. This approach requires the reformulation of the optimisation problem introduced in [8], since even both approaches are formulated as an integer optimization problem, isolability conditions considered in the former do not apply here. The novel aspects of the methodology are, first, the use of the nodal distances together with the sensitivity matrix at the sensor placement stage, in order to face the problem of mislabelling between leak signatures, which occurs in case of DMAs with a high number of nodes and a low number of sensors. Also, the sensitivities used to obtain the correlation between leak signatures are non-binary in order to avoid loss of information. The main aim is to reduce the effect of the leak mislabelling at the sensor placement stage, trying to geographically cluster nodes with similar leak signature. Hence, the sensor distribution promoting this behaviour is selected, and the rest are discarded. Work in the same direction has been done in the evolution between [19] and [18] at the leak location stage. In contrast with [19], in [18] the binarisation of the leak signature has been avoided in order to prevent the aforementioned loss of information. However, for a reduced number of sensors, the problem of mislabelling in large DMAs is still present. This is the reason why in this work this problem is targeted in a previous stage, i.e. sensor placement stage.[12] The second novel aspect presented here is the proposal of an assessment methodology using new figures of merit in order to provide the goodness of a certain sensor set from the leak location point of view, which is the next step after the sensors are placed. The assessment indices proposed assume that the leak location algorithm will be based on the correlation between leak signatures, but are independent of the methodology used in order to place the sensors, taking into account the intrinsic leak mislabelling that may occur in case of real DMAs with a low ratio between available sensors and network nodes, which may jeopardise the leak location. To the knowledge of the authors, the use of a general assessment in terms of potential number of isolated leaks is not present in the literature. In [10], an assessment based on the isolation distance is presented in a real DMA, but this do not include the goodness of the sensor distribution regarding the number of isolable leaks for the whole network.[13][14] Furthermore, the non-linear integer nature and the large dimension of the resulting optimisation problem calls for the use of an optimisation tool able to handle a problem with such features. A well-suited approach to handle this problem is the one based on Genetic Algorithms (GAs) [20, 21]. GAs are widely-used optimisation methods based on heuristics which mimic the natural evolution, such as crossover, mutation or inheritance. This is performed by means of a fitness function which selects the best individuals among different generations in order to provide an optimal solution to an specific problem.[15] The methodology presented is first illustrated in a small example and then evaluated in several DMAs, located in the Barcelona network.

The paper is organized as follows: the leak location[16] methodology used as the basis for this work is introduced in Section 2. The sensor placement methodology is presented in Section 3, and the isolability assessment used to evaluate the goodness of the sensor set proposed is introduced in Section 4. The application case studies, based on several DMAs, and the results obtained applying the methodology proposed are shown in Section 5. Finally, in Section 6, some concluding remarks and future work are given.

[9] R4-C4
[10] R4-C4
[11] R4-C4
[12] R2-C5
[13] R2-C8
[14] R2-C2, R2-C14, R5-C2
[15] R4-C8
[16] R4-C4

2. Leak Location[17] Problem

The leak location[18] problem may be separated in two different stages, which correspond to the sensor placement and the leak location[19] itself, given a set of sensors. The leak location approach is summarised in this section, since it is the basis of the sensor placement algorithm formulation proposed in this work.

The leak location methodology considered here aims to locate leaks within a DMA by means of some pressure measurements gathered from the network and their estimations obtained by a network hydraulic model. For a given DMA with N demand nodes and M pressure sensors, the leak detection methodology relies on the computation of the residuals $\mathbf{r} = [r_1 \ \dots \ r_M]^T$, where $r_i \in \mathbf{r}$ is the difference between the pressure measurement p_i and its corresponding estimation $\hat{p}_i$ obtained from a leakless simulation using the corresponding network hydraulic model as follows

$$r_i = p_i - \hat{p}_i, \quad i = 1, \dots, M \tag{1}$$

having one residual per each available pressure measurement within the DMA.

On the other hand, the leak location[20] method relies on the study of the residual vector in (1) by means of sensitivity analysis, aiming to determine the effect of each particular leak on every available pressure sensor measurement at a certain time [7]

$$\mathbf{S} = \begin{pmatrix} s_{11} & \cdots & s_{1N} \\ \vdots & \ddots & \vdots \\ s_{M1} & \cdots & s_{MN} \end{pmatrix} \tag{2}$$

given $M \leq N$ sensors within the network and N possible faults (assuming leaks only in nodes) with

$$s_{ij} = \frac{\hat{p}_{ij} - \hat{p}_i}{f_j}, \quad i = 1 \dots M, j = 1 \dots N \tag{3}$$

where $\hat{p}_i$ is the leakless scenario pressure estimation in node i and $\hat{p}_{ij}$ is the pressure estimation in node i due to leak f_j scenario occurring in node j.

To obtain the sensitivity matrix $\mathbf{S}$, a leak scenario per each node is generated by numerical simulation using EPANET hydraulic solver [22], obtaining the sensitivity vector corresponding to one column of the sensitivity matrix $\mathbf{S}$ as follows

$$\mathbf{s}_j = \begin{bmatrix} s_{1j} \\ \vdots \\ s_{Mj} \end{bmatrix}, \quad j = 1, \cdots, N \tag{4}$$

which is also known as leak signature[21]. Each simulated fault scenario is performed by setting a leak of magnitude f_j in the j^{th} DMA network node. This procedure is repeated for all the N existing network nodes. Then, matching both the residual vector in (1) and the sensitivity vectors in (4), leak location[22] may be performed by checking which node has the highest potential to present a leak. This analysis may be performed by using different metrics [23]. Here, a method presented in [18, 10], based on the correlation between residual and sensitivity vectors, is considered. According to the study in [9], this[23] method presents the best performance for leak location, even it should be remarked that the sensor placement method presented in this paper could be applied with alternative leak location methods exploiting sensitivity analysis.

[17] R4-C4
[18] R4-C4
[19] R4-C4
[20] R4-C4
[21] R4-C10
[22] R4-C4
[23] R4-C9

The current metric considered here for leak location[24] is based on the correlation function given by the inner product of the regressor vector in (1) and the sensitivity vector in (4), for each particular fault in node j

$$\gamma_j = \frac{\mathbf{s}_j{}^T \mathbf{r}}{|\mathbf{s}_j||\mathbf{r}|}. \tag{5}$$

Then, the highest correlation determines the candidate leaky node k

$$\gamma_k = \max(\gamma_1, \cdots, \gamma_N). \tag{6}$$

The objective here is to develop a methodology to place a given number of sensors, M, within a DMA in order to obtain a sensor set maximizing leak isolability under realistic conditions. In DMAs with a large number of nodes, the sensitivity to different leaks occurring in different nodes may be very similar. This sensitivity similarity may lead to confusion between different leaks when a low number of sensors is available and uncertainty in the measurements and in the model is present, which is generally the actual situation. This situation may be solved e.g. by increasing the number of sensors, in order to increase the dimension of the leak signature, or by selecting these measured nodes with a methodology preventing sensitivity similarity for the different leak scenarios considered, as suggested by the methodology presented here. This methodology relies on the leak location scheme presented in this section.[25] This is the first stage of the twofold leak location[26] problem, where leaks are located given a set of sensors at the second stage. The methodology to obtain this sensor set, based on the correlation-based method presented here, is introduced in the next section.

3. Sensor Placement Methodology

3.1. Sensor Placement as an Optimisation Problem

The goal here is to place the best sensor set in order to locate the leak as precisely as possible within the considered water network. The sensor distribution method is based on the system sensitivity matrix (2). As discussed in the introduction, a former methodology is presented in [8], where the residuals are binarized by a certain threshold value. In the approach presented here, the complete information of the residual is used in order to avoid data loss and hence to increase leak discriminability [18]. Also, the sensor placement method uses a relaxed isolation index to better handle some real-world effects affecting water network systems, such as system non-linearity, sensor measurements resolution and model uncertainty (e.g. in the demands or network element parameters). These real-world effects cause deviation between the modelled and the actual system behavior, which may lead to mislabel the latter, and the confusion between different leak scenarios (sensitivity vectors in (4)). However, if the confusion involves geographically close behaviors, these undesired effects do not severely impact the final leak location[27]. Hence, the optimal sensor distribution takes into account that the leak location[28] distance may be relaxed and places the sensors accordingly in order to geographically cluster leaks with similar signature (4). In order to perform the sensor placement of M sensors, let us define the binary decision vector that represents the selected sensors

$$\mathbf{x} = \begin{pmatrix} x_1 & \cdots & x_N \end{pmatrix}^T \tag{7}$$

where $x_i = 1$ if the pressure sensor in node i is installed and 0 otherwise. Defining

$$\mathbf{X}(\mathbf{x}) = diag(x_1, \cdots, x_N) \tag{8}$$

the corresponding sensitivity vectors can be represented as follows

$$\bar{\mathbf{s}}_j(\mathbf{x}) = \mathbf{X}(\mathbf{x})\mathbf{s}_j, \quad j = 1, \cdots, N \tag{9}$$

[24] R4-C4
[25] R2-C15
[26] R4-C4
[27] R4-C4
[28] R4-C4

where $\mathbf{s}_j$ is the sensitivity matrix obtained when all the N sensors are available, i.e. $M = N$. Hence, the projection between two different leak signatures[29] i and j for a given subset of sensors $\mathbf{x}$ is introduced by their inner product as follows

$$\gamma_{ij}(\mathbf{x}) = \frac{\bar{\mathbf{s}}_i^T(\mathbf{x})\bar{\mathbf{s}}_j(\mathbf{x})}{|\bar{\mathbf{s}}_i(\mathbf{x})||\bar{\mathbf{s}}_j(\mathbf{x})|} = \frac{\mathbf{s}_i^T\mathbf{X}(\mathbf{x})\mathbf{s}_j}{|\mathbf{X}(\mathbf{x})\mathbf{s}_i||\mathbf{X}(\mathbf{x})\mathbf{s}_j|}, \quad i, j = 1, \cdots, N \tag{10}$$

where $\bar{\mathbf{s}}_i, \bar{\mathbf{s}}_j$ are vectors corresponding to two different fault signatures (columns) for each class (leak) in the sensitivity matrix (2) and γ_{ij} is a measure of similarity between these two classes. From (10), the projection matrix may be stated as follows

$$\Gamma(\mathbf{x}) = \begin{pmatrix} \gamma_{11}(\mathbf{x}) & \cdots & \gamma_{1N}(\mathbf{x}) \\ \vdots & \ddots & \vdots \\ \gamma_{N1}(\mathbf{x}) & \cdots & \gamma_{NN}(\mathbf{x}) \end{pmatrix}. \tag{11}$$

Regarding the nature of its elements, the matrix derived in (11) is called cross-correlation matrix. It may be noted that the latter is symmetric, so $\Gamma = \Gamma^\top$.

In order to evaluate the quality of a sensor allocation setup, $\rho_{ij}(\mathbf{x})$ is defined

$$\begin{aligned} \rho_{ij}(\mathbf{x}) = &\left(\gamma_{ij}(\mathbf{x})\left(1 - \frac{d_{ij}}{d_{\max}}\right)\right)^{d_c} \\ &+ \left(\left(1 - \gamma_{ij}(\mathbf{x})\right)\frac{d_{ij}}{d_{\max}}\right)^{d_f}, \quad i, j = 1 \ldots N \end{aligned} \tag{12}$$

where γ_{ij} is the cross-correlation between leak i and leak j signature vectors, d_{ij} is the topological (pipe) distance between leaky nodes i and j, $d_{\max}$ is the maximum pipe distance for the whole network and d_c and d_f are tuning parameters related with the included high-correlated close leaks cluster and the excluded high-correlated distant leaks for a given i-j leak pair, respectively.[30] This particular cost function aims to obtain the best sensor set in order to locate the leaky node as precisely as possible, grouping leaks with similar correlation as geographically close as possible, whilst discarding sensor sets promoting leaks with similar signature in distant locations. On the one hand, parameter d_c is related with the isolation zone, i.e. the zone in which we allow leaks to be mislabelled. An acceptable value for the perimeter is about 200 m in a real DMA, and is provided by the company managing the network. Inside this perimeter, other on-the-ground techniques (e.g. ground penetrating radar) are used for finer isolation. Hence, d_c is selected accordingly, i.e. making the cost function decrease its value when distance to most correlated leak is below the selected perimeter, also taking into account the corresponding DMA $d_{\max}$. On the other hand, parameter d_f is related with the exclusion zone, i.e. the zone where leaks should not be mislabelled with the leaks in the isolation zone. Hence, d_f is selected such that outside the inclusion zone leak mislabelling is penalized, i.e. the cost function decreases its value when distance is above the selected perimeter and correlation with the potential leak occurring increases. The values of d_c and d_f parameters should be selected such that (12) range from zero to one for each i-j leak pair. These parameters may also be used to adjust the target of the optimisation. The bigger d_c, d_f, the narrower the related zone. Generally d_c is chosen bigger than d_f so the slope of the exclusion term is lower, since the exclusion zone embraces all the nodes in the network outside the inclusion perimeter. However, if one wants to get focused on the leak isolation zone, d_f may be chosen arbitrarily high in order to penalise arbitrarily distant nodes.[31]

Considering (12), the sensor placement may be stated as an optimisation problem, with the following cost function

[29] R4-C10
[30] R2-C16, R4-C11
[31] R2-C12, R2-C13, R4-C11

$$\rho(\mathbf{x}) = 1 - \frac{1}{N^2}\sum_{i=1}^{N}\sum_{j=1}^{N}\rho_{ij}(\mathbf{x}). \tag{13}$$

As shown in (13), (12) is obtained for all the N^2 *i-j* node pairs and normalized, so (13) range from zero to one.[32] Then, the optimisation problem may be formulated as follows

$$\begin{aligned} \underset{\mathbf{x}}{\text{minimize}} \quad & \rho(\mathbf{x}) \\ \text{subject to} \quad & \sum_{i=1}^{N}\mathbf{x}_i = M \end{aligned} \tag{14}$$

where $\rho(\mathbf{x})$ is to be optimised over the full N sensors set available, and M is a predefined restriction on the number of sensors to install. The cost function in (13) for a single *i-j* leak pair is depicted in Figure 1 for illustrative purposes.[33] The criterion to select the parameters d_c and d_f may be illustrated with Figure 1b, for a DMA with $d_{\max} = 1000$ m. Parameter d_c is selected so γ_{ij} starts decreasing at a normalised distance $d_{ij}/d_{max} = 0.2$, corresponding to a distance of 200 m. Similar criterion is applied for the selection of d_f, related with the leak exclusion area.[34] Hence, the use of this cost function aims to achieve a sensor distribution obtaining high-correlation/low-distance (first term in (12)) and low-correlation/high-distance (second term in (12)) leak scenario combinations.

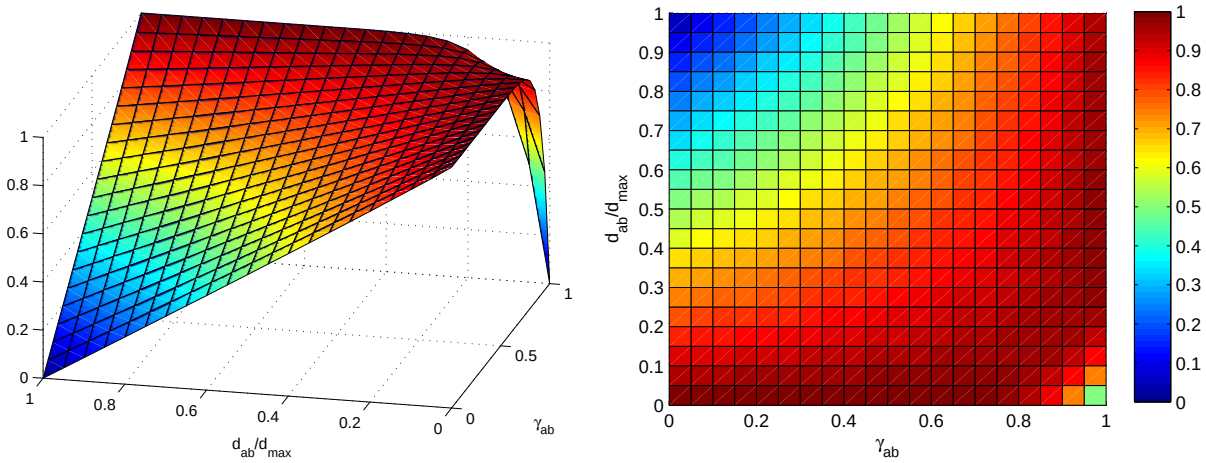

(a) (b)

Figure 1: Cost function for a single $i - j$ pair

The sensor placement optimisation problem (14) is solved using GA, which is a suitable approach for large-scale binary non-linear problems as the one considered here [24]. Further details on the GA parameters utilised to solve this particular problem are given in Section 5.2[35].

4. Isolability Assessment[36]

In order to assess the fault isolability capabilities of a fault isolation method considering a particular set of measurement points and a given topology, a metric based on the confusion matrix is used [25]. The confusion matrix is

[32] R4-C13
[33] R2-C6, R4-C12
[34] R2-C12
[35] R2-C17
[36] R2-C18

a specific table layout which allows the visualisation of the performance achieved by a certain fault diagnosis layout, i.e. a certain sensor set and its corresponding sensitivity model. Each column of this matrix represents instances in a predicted class/fault, whilst each row stands for instances in an actual class/fault. The name stems from the fact that this representation allows to check when the fault diagnosis method is confusing two different classes, commonly by mislabelling one as another. A confusion matrix displays the number of correct and incorrect predictions made by the fault isolation model compared with the actual class occurring in the test data. Here, a variation of the confusion matrix is presented in (15) in order to show the mislabelling between different leaks by comparing the predicted classes against themselves[37]

$$C = \begin{pmatrix} \kappa_{11} & \cdots & \kappa_{1N} \\ \vdots & \ddots & \vdots \\ \kappa_{N1} & \cdots & \kappa_{NN} \end{pmatrix} \tag{15}$$

where $\kappa_{ij} \in \{0, 1\}$ for $i, j = 1 \dots N$. Matrix in (15) shows how the fault isolation model obtained by a certain sensor set is mislabelling different faults between two different nodes i and j, which could be confused according to the considered metric. The values of κ_{ij} depend on each particular isolation criterion used. Here, a criterion based on the cross-correlation (11) is used to obtain the maximum correlation for each actual fault

$$\gamma_{ij_{\max}} = \max_{j \in 1 \dots N} \gamma_{ij}, \quad i = 1 \dots N \tag{16}$$

being κ_{ij} as follows,

$$\kappa_{ij} = \begin{cases} 1 & \gamma_{ij} = \gamma_{ij_{\max}} \\ 0 & \text{otherwise} \end{cases}, \quad i, j = 1 \dots N. \tag{17}$$

Hence, the matrix (15) is called confusion cross-correlation matrix here. In order to provide less conservative isolation results while still realistic and well suited to the optimisation criterion stated in (14)[38], the matrix of pipe distances among nodes of the network may be presented

$$D = \begin{pmatrix} d_{11} & \cdots & d_{1N} \\ \vdots & \ddots & \vdots \\ d_{N1} & \cdots & d_{NN} \end{pmatrix} \tag{18}$$

and the isolation condition in (17) may be relaxed by a certain fault isolation cluster distance d_{cluster} as follows

$$\kappa_{ij} = \begin{cases} 1 & \max \mathbf{d}_{ij_{\max}} < d_{\text{cluster}} \quad \text{and} \quad d_{ij} < \max \mathbf{d}_{ij_{\max}} \\ 0 & \text{otherwise} \end{cases}, \quad i, j = 1 \dots N \tag{19}$$

where $\mathbf{d}_{ij_{\max}}$ is the distance between the actual faulty node i and the node (or nodes) with highest correlation $\gamma_{ij_{\max}}$ (i.e. predicted faulty nodes), and d_{cluster} is the maximum allowed distance between the actual faulty node i and the predicted faulty nodes, in order to consider the leak in i is well isolated. When several predicted faulty nodes are obtained, the worst case (i.e. $\max \mathbf{d}_{ij_{\max}}$) is considered.[39]

The number of correctly isolated faults is given by the isolation index[40]

$$\zeta = \text{tr}\,(C) \tag{20}$$

[37] R2-C19
[38] R4-C14
[39] R4-C15, R2-C20
[40] R4-C17

so the correct isolated faults are those which are assigned to its own class and not to any other possible fault occurring in the system. The best isolation index[41] (ζ_{best}) for a given d_{cluster} is obtained when sensors in all nodes are available i.e. when $M = N$, which states a topological limit

$$0 \leq \zeta_{opt} \leq \zeta_{best} \leq N \tag{21}$$

where ζ_{opt} is the isolation index obtained with the corresponding optimal sensor placement, for a given d_{cluster}. Let us also define a particular ζ_{opt} and ζ_{best} considering (17), i.e. ζ_{opt_0} and ζ_{best_0}, respectively. Then, a more general topological limit which does not depend on the distance between nodes may be given by

$$0 \leq \operatorname{rank} \mathbf{S} \leq \zeta_{opt_0} \leq \zeta_{best_0} \leq N \tag{22}$$

where $\mathbf{S}$ is the sensitivity matrix obtained when all the N sensors are available, i.e. $M = N$. Relation in (22) is meaningful since ζ_{best_0} computation may be infeasible for DMAs with a high number of nodes N. Then, $\operatorname{rank} \mathbf{S}$ may provide a useful computationally efficient approximation, specially when this magnitude is close to the DMA number of nodes N. It must be noted that, since matrix $\mathbf{S}$ is affected by the pressure sensor resolution, confusion between leaks may be induced (e.g. linear dependency between columns of $\mathbf{S}$) as the DMA size increases.[42]

It may also be noted that the ratio $\phi_{best} = \frac{\zeta_{best}}{\zeta_{best_0}} \geq 1$ suggests the benefit obtained by the geographic relaxation when all the sensors are available (the bigger the better), whilst the ratio $\phi_{opt} = \frac{\zeta_{opt}}{\zeta_{opt_0}} \geq 1$ suggests the geographical relaxation benefit for the sensor subset considered. This benefit may be also obtained from an extra coverage percentage over ζ_{best} as follows

$$\delta = \frac{\zeta_{opt} - \zeta_{opt_0}}{\zeta_{best}} 100 \tag{23}$$

where δ is the percentage of extra coverage over ζ_{best} obtained when geographically relaxing the assessment.

5. Application Examples: Hanoi and Barcelona Drinking Water Networks

5.1. Description

Several DMAs of different level of complexity are used here in order to show the performance of the method presented. First, a reduced DMA is considered to illustrate the method. The Hanoi DMA, an existing benchmark network widely used in the literature (see, e.g. [26]), is considered for this purpose (Figure 2). This DMA has 31 nodes and 34 links, and delivers water to the end consumers by means of a single input point. Also, two different DMAs located in the Barcelona area, with higher nodal density, are used as case studies (Figure 3).[43] On the one hand, the *Canyars* DMA (Figure 4) is located at the pressure level 80 within the Barcelona water supply network. This DMA has 694 nodes and 719 links, and delivers water to the end consumers by means of a single input point. On the other hand, the *Castelldefels Platja* DMA (Figure 5) is located at the pressure level 50 within the Barcelona water supply network. This DMA has 4952 nodes and 5116 links, and covers an area of 606 ha. The DMA has two inputs (Ferrocarril and Pi Tort) delivering water to the end consumers. The current DMA size motivated its reduction to an equivalent hydraulic model of 2828 nodes using skeletonization techniques [27], more suitable for high demanding computation algorithms involved here.

In order to simulate these DMAs isolated from the water supply network, the boundary conditions (i.e. pressure and flow measurements from the network) are fixed. Generally, pressure is fixed using a reservoir and the overall demand is obtained as the sum of the inflow distributed through the DMA using a demand pattern model. The total inflow is distributed using a constant coefficient (base demand) in each consumption node. Hence, all the consumptions are assumed to share the same profile, whilst the billing information is used to determine the base demand of each particular consumption. A good estimation of the demand model is paramount for the real case application.

[41] R4-C17
[42] R4-C18
[43] R2-C10

5.2. Results

In this section, the results achieved applying the sensor placement methodology described in Section 3 are presented. The sensors considered here are pressure sensors which may be installed in any node of the network. The maximum isolation distance d_{cluster}, which is a parameter given by the company managing the network, is assumed of 200 m for the DMAs in Section 5.2.2 and Section 5.2.3, whilst is assumed of 2000 m for the illustrative DMA in Section 5.2.1 due to its particularly low nodal density. For distances below d_{cluster}, there exist alternative more precise methods to isolate the leak e.g. ground penetrating radar. Scenarios have been generated using EPANET hydraulic simulation software, as introduced in Section 2.

Regarding GA parameters, an initial population of 100 random sensor sets, including the potential sensors to be used, is employed to seed the GA algorithm. At this stage, already installed DMA sensors may be included to seed the GA. The number of individuals in each generation is set to 100, the maximum number of generations allowed is set to 30, the termination tolerance on the fitness function value is set to 1×10^{-6} and the number of generations over which cumulative change in fitness function value is less than the termination tolerance (stall generations limit) is set to eight. Since the optimum obtained by the GA is not global, consecutive GA optimisations are conducted until fitness function value do not improve between two overall optimisations, aiming to achieve the best possible solution. The selection of these parameters takes into account that the optimisation is dealing with real high dimension DMAs and the problem may be computationally intensive. In order to face such computational issues, the use of local parallel computing is used when multiple labs are available in the host PC, in order to increase computation power. The host PC implemented Intel® Core™ i7 Quad-Core processors and 8 GB of 1600 MHz Dual Channel DDR3 memory, which allowed the use of such technique.[44]

5.2.1. Hanoi DMA

The sensor placement results obtained considering Hanoi DMA (Figure 2) are depicted in Figures 7a to 7d. The sensitivity matrix $\mathbf{S}$ is obtained for a 24 h scenario using an emitter coefficient (i.e. discharge coefficient for emitter placed at junction, representing the flow in liters per second (LPS)[45] occurring at a pressure drop of 1 psi [22]) of 5 LPS/psi$^{0.5}$. The sensitivity $\mathbf{S}$ is concatenated for the 24 hours available, leading to a dimension of 744×31. The distance used here is the topological distance among nodes, i.e. minimum pipe distance between these elements. This network has a low density of nodes per squared meter, being the minimum distance among the closest nodes of 484 m. Hence, d_{cluster} should be increased in comparison to a regular network, in order to provide realistic results. For this particular network, the maximum number of isolable faults considering all the sensors available (ζ_{best_0}) is 31, and the maximum number of isolable faults considering all the sensors available and $d_{\text{cluster}} = 2000$ m (ζ_{best}) is 28 (90 % of $N = 31$ nodes forming the network), respectively. According to the specified d_{cluster} and $d_{\max} = 16426$ m, the cost function parameters have been chosen of $d_c = 5.36$ and $d_f = 0.57$.[46] The evolution of the GA optimisation for each sensor distribution is depicted in Figures 6a to 6d. In the lower row, the latter figures show the evolution of the average distance between individuals among generations in the bottom-left subplot, and the fitness of each individual in the last generation in the bottom-right subplot. In the upper row, the evolution of the best and mean fitness value per generation is depicted in the upper-left subplot, and the GA stopping criteria is depicted in the upper-right subplot. These include the generations limit (30) i.e. the maximum number of generations per optimisation, the time limit (unspecified) i.e. the maximum time in seconds whilst the GA runs before stopping, the stall generations limit (eight) i.e. the number of maximum consecutive generations without improving the average relative change in the best fitness function over a given function tolerance (1×10^{-6}) and the stall time limit (unspecified), i.e. the time interval in seconds after the GA stops if no improvement is obtained in the best fitness value. Time constraints have not been specified since they were not critical parameters in the optimisations. As it is shown in the Figures 6a to 6d, the stopping criteria met in all the optimisations for this particular case is the stall generation limit. Isolation assessment results concerning sensor distribution for different number of sensors (from two to five) are detailed in Table 1. It may be observed how the results obtained between four and five sensors do not improve in terms of ζ_{opt}, even a better ρ is achieved for five sensors at the optimisation stage. In this case, the benefit of installing extra sensors may

[44] R1-C1, R2-C12, R2-C17
[45] R4-C19
[46] R2-C12

Table 1: Isolation assessment results, Hanoi DMA

Number of sensors	2	3	4	5
ζ_{opt}	14	20	22	22
% of N	45	64.5	70.97	70.97
% of ζ_{best}	50	71.43	78.57	78.57
% of ζ_{best_0}	45	64.52	70.96	70.96
ζ_{opt_0}	30	31	31	31
ρ	0.6804	0.6586	0.6445	0.6426

obtain reduced isolation clusters, but still bigger than d_{cluster}. Hence, the optimal sensor distribution is obtained for four sensors (Figure 7c) since is the one achieving best ζ_{opt} with the minimum number of sensors. For the particular layout of this DMA, which is geographically large (d_{max} = 16426 m) but with low nodal density (N = 31 nodes, with minimum distance among closest nodes of 484 m), the geographical relaxation is not providing any particular benefit (δ is negative for all the distributions considered). However, the methodology presented here is useful when there exists leak signature confusion, which is not the case in this network ($\zeta_{opt} = N$ for almost all the sensor distributions considered). Hence, a network of this characteristics is useful for illustrative purposes, but it is not a target network for the proposed methodology, more intended to be used in larger DMAs found in real water networks as the ones presented in the following sections.[47]

5.2.2. *Canyars DMA*

The sensor placement results obtained when considering Canyars DMA (Figure 4) are depicted in Figures 8a to 8c. The sensitivity matrix **S** is obtained for a fixed leak of 6 LPS, in an hourly sampled scenario comprised between 24/02/2014 9h and 25/02/2014 9h. Thus, the sensitivity **S** is concatenated for the 24 hours available leading to a dimension of 16656 × 694. Also, the information in this matrix considers sensor resolution of 0.1 m in order to take into account current technological constraints in the simulated scenario. The distance used here is the topological distance among nodes, i.e. minimum pipe distance between these elements. For this particular network, the maximum number of isolable faults considering all the sensors available (ζ_{best_0}) is 399, and the maximum number of isolable faults considering all the sensors available and d_{cluster} (ζ_{best}) is 398 (57 % of N = 694 nodes forming the network). According to the specified d_{cluster} = 200 m and d_{max} = 888 m, the cost function parameters have been chosen of d_c = 8.31 and d_f = 1.04, respectively.[48]

Isolation assessment results concerning sensor distribution for different number of sensors (from two to four) are detailed in Table 2. It may be observed how the relaxation by d_{cluster} does not have much effect when having all the sensors available (i.e. $\phi_{best} \cong 1$), but it does for a limited sensor set (see Table 2) e.g. for two sensors, with ζ_{opt} = 267 and ζ_{opt_0} = 116, δ = 38 % extra coverage over ζ_{best} is achieved when geographically relaxing the assessment. It may also be observed how the results obtained between three and four sensors do not improve in terms of ζ_{opt}, even a better ρ is achieved for four sensors at the optimisation stage. In this case, the benefit of installing extra sensors may obtain reduced isolation clusters, but still bigger than d_{cluster}. Hence, since the coverage of the network is high (97 % of ζ_{best}), the optimal sensor distribution is obtained for three sensors (Figure 8b) since is the one achieving best ζ_{opt} with the minimum number of sensors.

The impact of sensors resolution is also worth to be noted. Although it does not have impact on the maximum number of isolable faults ζ_{best} = 398 (hence, the maximum achievable coverage is not limited by the sensors resolution but by the topological network setup, when sufficient number of sensors are available), it does have impact on ζ_{opt} for different sensor setups (hence, for limited information gathered from the network, sensor resolution effect is noticeable). For example, considering five full-resolution sensors setup, almost complete coverage of the network is achieved (ζ_{opt} = 395), against the 388 isolable faults achieved by the five limited-resolution (0.1 m) sensors setup counterpart.

[47] AE-C1, R2-C10
[48] R2-C12

Table 2: Isolation assessment results, Canyars DMA

Number of sensors	2	3	4
ζ_{opt}	267	388	388
% of N	38	56	56
% of ζ_{best}	67	97	97
% of ζ_{best_0}	67	97	97
ζ_{opt_0}	116	242	245
ρ	0.7375	0.7342	0.7321

Table 3: Isolation results, Castelldefels Platja DMA

Number of sensors	4	5	6
ζ_{opt}	2649	2665	2665
% of N	93.67	94.24	94.24
% of ζ_{best}	93.8	94.37	94.37
% of rank $\mathbf{S}$	93.67	94.24	94.24
ζ_{opt_0}	902	982	1067
ρ	0.5116	0.5086	0.5071

5.2.3. *Castelldefels Platja DMA*

The sensor placement results obtained considering *Castelldefels Platja* network (Figure 4) are depicted in Figures 9a to 9c. The sensitivity matrix $\mathbf{S}$ is obtained for an emitter coefficient of 0.92 LPS/psi$^{0.5}$, in an hourly sampled scenario comprised between 24/02/2014 9h and 25/02/2014 9h, so $\mathbf{S}$ is concatenated for the 24 hours available and is of dimension 67872 x 2828. Also, the information in this matrix is truncated by sensor resolution (i.e. 0.1 m). The distance used here is the topological distance among nodes, i.e. minimum pipe distance between these elements. For this particular network, the computation of ζ_{best_0} is not possible due to computational issues related with network size N, as introduced in Section 4. Alternatively, the rank of $\mathbf{S}$ is used, providing a maximum number of isolable faults approximation considering all the sensors available, that is 2828. Since this value is close to N, it may be considered a feasible approximation of the maximum number of isolable faults. Also, the maximum number of isolable faults considering all the sensors available and d_{cluster} (ζ_{best}) is 2824 (the 99.9 % of N = 2828 nodes forming the network). It may be observed how the relaxation by d_{cluster} does not either have much impact in this DMA when having all the sensors available (i.e. $\phi_{best} \approxeq 1$), but it does as in Canyars DMA when limited number of sensors are available (see Table 3) e.g. for four sensors, with ζ_{opt} = 2649 and ζ_{opt_0} = 902, δ = 62 % extra coverage over ζ_{best} is achieved when geographically relaxing the assessment. According to the specified d_{cluster} = 200 m and $d_{\max}$ = 7222 m, the cost function parameters have been chosen of d_c = 6.41 and d_f = 0.46, respectively.[49]

Isolation assessment results concerning sensor distribution for different number of sensors considered (from four to six) are detailed in Table 3. It may be seen how for five and six sensors, the number of isolable faults for the optimal sensor set (ζ_{opt}) equals 2665, so according to the criterion no advantage is obtained from the usage of this extra sensor. Hence, the number of suggested sensors for this network is five (Figure 9b), achieving a theoretical coverage of the 94.24 % of the total possible faults.

6. Conclusions

In this paper, a successful sensor placement and leak location[50] assessment methodologies are proposed in order to improve the performance of leak location[51] in water distribution networks, which may have severe impact on maintenance costs and performance of the water distribution along DMAs. Common problems arising on the leak

[49] R2-C12
[50] R4-C4
[51] R4-C4

diagnosis in large real water networks can be addressed at the sensor placement stage, e.g. leak discriminability and large location[52] areas, when taking into account real world leak diagnosis trade-offs related with geographic location[53] precision. Hence, a general method of sensor placement is proposed, taking into account these trade-offs by clustering similar leaks geographically within an acceptable location[54] area from the application point of view. The proposed method achieved promising leak location[55] results, evaluated by an also proposed general assessment method for leak diagnosis in water distribution systems, in a small illustrative DMA in Hanoi and two DMAs situated in the Barcelona urban area. These results motivate the use of the proposed methodology in the actual and similar water networks. Further work involves the inclusion of the number of sensors to install as part of the optimisation problem, as well as the consideration of uncertainty (e.g. in sensor measurements and demand model) in the sensor placement algorithm to cope with more realistic assumptions. Also, the extension to multiple leak scenarios may be considered in future steps of this work, by e.g. developing further methods in order to expand the sensitivity matrix accordingly, taking into account that the selection of these new scenarios should be performed carefully in order to avoid computational issues derived from handling high dimension matrices.[56]

Acknowledgement

This work has been partially funded by the Spanish Ministry of Science and Technology through the Project ECOCIS (Ref. DPI2013-48243-C2-1-R) and Project HARCRICS (Ref. DPI2014-58104-R), and by EFFINET grant FP7-ICT-2012-318556 of the European Commission. The authors also wish to thank the support received by the Water Technological Center (CETAQUA) of the company managing the Barcelona water network (AGBAR).

References

[1] Y. Khulief, A. Khalifa, R. Mansour, M. Habib, Acoustic detection of leaks in water pipelines using measurements inside pipe, Journal of Pipeline Systems Engineering and Practice 3 (2) (2012) 47–54.
[2] M. Lambert, A. Simpson, J. Vitkovsky, X.-J. Wang, P. Lee, A review of leading-edge leak detection techniques for water distribution systems, in: 20th AWA Convention, Perth, Australia, 2003.
[3] R. Puust, Z. Kapelan, D. A. Savic, T. Koppel, A review of methods for leakage management in pipe networks, Urban Water Journal 7 (1) (2010) 25–45.
[4] A. Lambert, What do we know about pressure leakage relationships in distribution systems?, in: IWA Conference System Approach to leakage control and water distribution system management, no. May, Brno, Czech Republic, 2000, pp. 1–9.
[5] J. Thornton, A. Lambert, Progress in practical prediction of pressure: leakage, pressure: burst frequency and pressure: consumption relationships, in: Leakage Conference Proceedings, Halifax, Canada, 2005, pp. 1–10.
[6] A. F. Colombo, P. Lee, B. W. Karney, A selective literature review of transient-based leak detection methods, Journal of Hydro-environment Research (2009) 212–227.
[7] R. S. Pudar, J. A. Liggett, Leaks in pipe networks, Journal of Hydraulic Engineering 118 (7) (1992) 1031–1046.
[8] R. Pérez, V. Puig, J. Pascual, J. Quevedo, E. Landeros, A. Peralta, Methodology for leakage isolation using pressure sensitivity analysis in water distribution networks, Control Engineering Practice 19 (10) (2011) 1157 – 1167. doi:10.1016/j.conengprac.2011.06.004.
[9] M. V. Casillas, L. Garza-Castañón, V. Puig, Model-based leak detection and location in water distribution networks considering an extended-horizon analysis of pressure sensitivities, Journal of Hydroinformatics 16 (2014) 649–670.
[10] R. Pérez, M. A. Cugueró, J. Cugueró, G. Sanz, Accuracy assessment of leak localisation method depending on available measurements, Procedia Engineering 70 (2014) 1304–1313. doi:10.1016/j.proeng.2014.02.144.
[11] A. Yassine, S. Ploix, J. M. Flaus, A method for sensor placement taking into account diagnosability criteria, International Journal of Applied Mathematics and Computer Science 18 (4) (2008) 497–512. doi:10.2478/v10006-008-0044-5.
[12] A. Rosich, R. Sarrate, F. Nejjari, Optimal sensor placement for FDI using binary integer linear programming, in: 20th International Workshop on Principles of Diagnosis, DX09, 2009, pp. 235–242.
[13] A. Krause, J. Leskovec, C. Guestrin, J. Vanbriesen, C. Faloutsos, Efficient sensor placement optimization for securing large water distribution networks, Journal of Water Resources Planning and Management 134 (6) (2008) 516–526.
[14] M. Aral, J. Guan, M. Maslia, Optimal design of sensor placement in water distribution networks, Journal of Water Resources Planning and Management 136 (1) (2010) 5–18.
[15] R. Sarrate, F. Nejjari, A. Rosich, Sensor placement for fault diagnosis performance maximization in distribution networks, in: Control & Automation (MED), 2012 20th Mediterranean Conference on, 2012, pp. 110–115.

[52] R4-C4
[53] R4-C4
[54] R4-C4
[55] R4-C4
[56] R2-C4, R4-C5

[16] S. Christodoulou, A. Gagatsis, A. Xanthos, S. Kranioti, A. Agathokleous, M. Fragiadakis, Entropy-based sensor placement optimization for waterloss detection in water distribution networks, Water Resources Management 27 (13) (2013) 4443–4468.
[17] M. Farley, S. Trow, Losses in Water Distribution Networks, IWA publishing, London, 2003.
[18] J. Quevedo, M. A. Cugueró, R. Pérez, F. Nejjari, V. Puig, J. M. Mirats, Leakage location in water distribution networks based on correlation measurement of pressure sensors, in: 8th IWA Symposium on System Analysis and Integrated Assessment (Watermatex), International Water Association (IWA), San Sebastián, 2011, pp. 290–297.
[19] R. Pérez, V. Puig, J. Pascual, A. Peralta, E. Landeros, L. Jordanas, Pressure sensor distribution for leak detection in Barcelona water distribution network, Water Science & Technology: Water Supply 9 (6) (2009) 715 – 721. doi:10.2166/ws.2009.372.
[20] C. R. Reeves (Ed.), Modern Heuristic Techniques for Combinatorial Problems, Mcgraw Hill, UK, 1995.
[21] J. R. Koza, Survey of genetic algorithms and genetic programming, Proceedings of 1995 WESCON Conference (1995) 589–594.
[22] L. A. Rossman, EPANET 2 Users Manual, Environmental Protection Agency (EPA), U.S. (September 2000).
[23] L. Rokach, O. Maimon, Clustering methods, in: Data Mining and Knowledge Discovery Handbook, 2005, pp. 321–352.
[24] K. Gallagher, M. Sambridge, Genetic algorithms: A powerful tool for large-scale nonlinear optimization problems, Computers & Geosciences 20 (7-8) (1994) 1229–1236.
[25] T. Fawcett, An introduction to ROC analysis, Pattern Recognition Letters 27 (8) (2006) 861–874.
[26] M. V. Casillas-Ponce, L. E. Garza-Castañón, V. Puig-Cayuela, Model-based leak detection and location in water distribution networks considering an extended-horizon analysis of pressure sensitivities, Journal of Hydroinformatics 16 (3) (2014) 649–670. doi:10.2166/hydro.2013.019.
[27] T. Walski, D. Chase, D. Savic, W. Grayman, S. Beckwith, E. Koelle, Advanced Water Distribution Modeling and Management, Haestad Press, 2003.

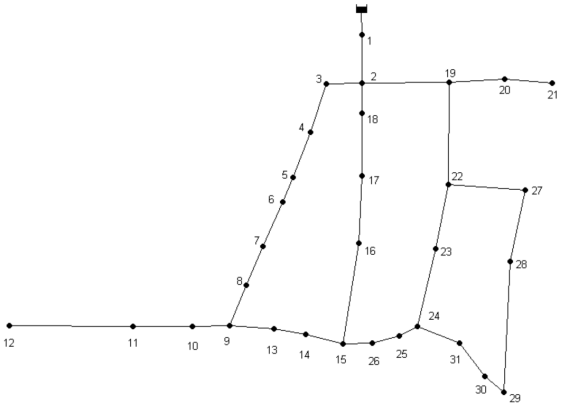

Figure 2: Hanoi DMA

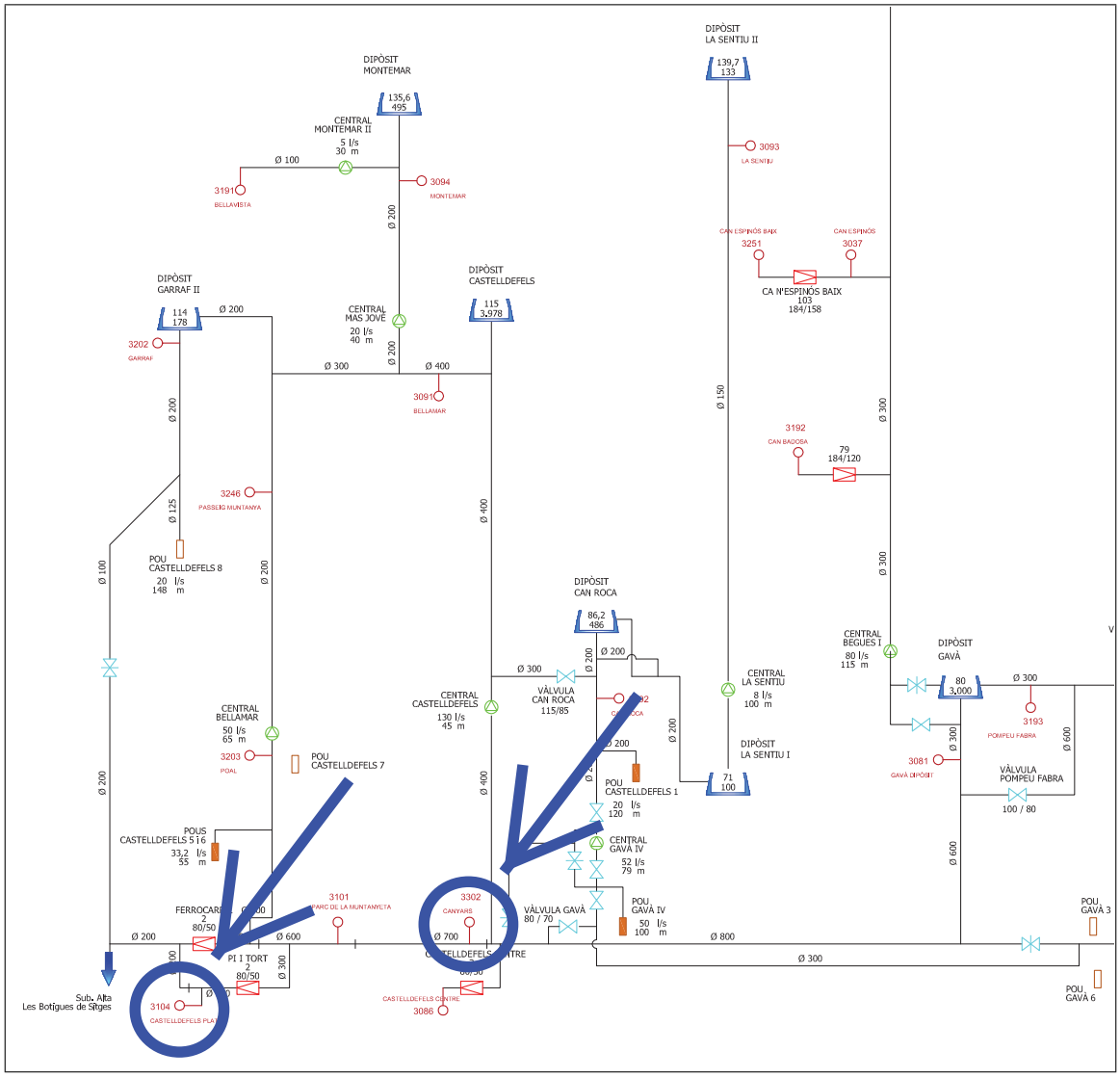

Figure 3: Barcelona Drinking Water Supply Network detail (arrows: Castelldefels Platja and Canyars DMAs, respectively)

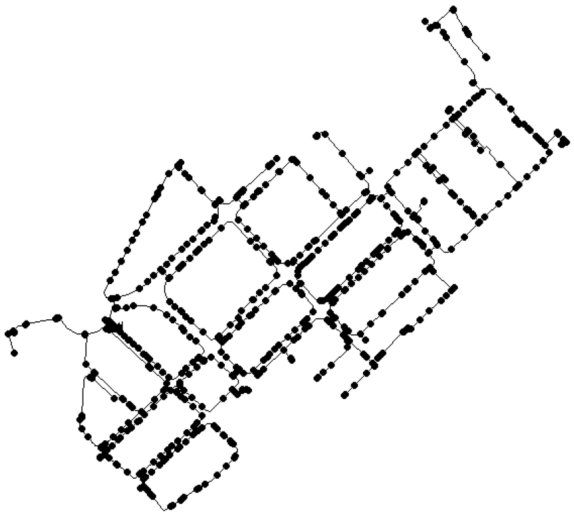

Figure 4: Canyars DMA

Figure 5: Castelldefels Platja DMA

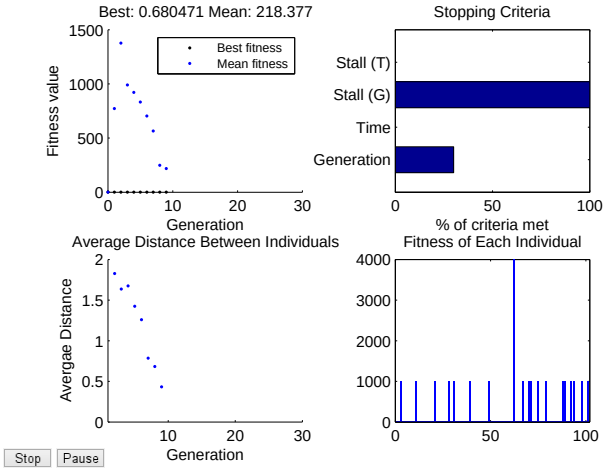

(a) Two sensors

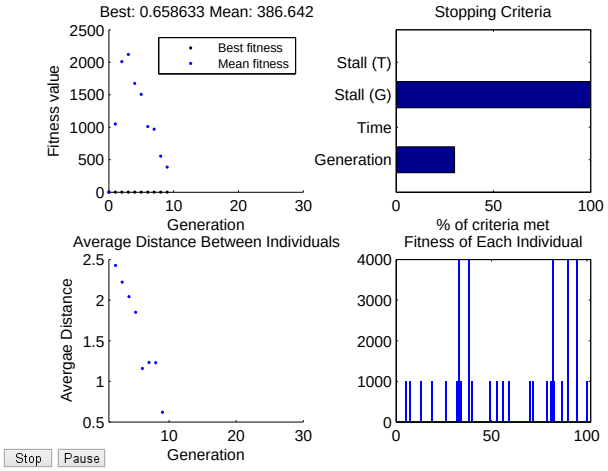

(b) Three sensors

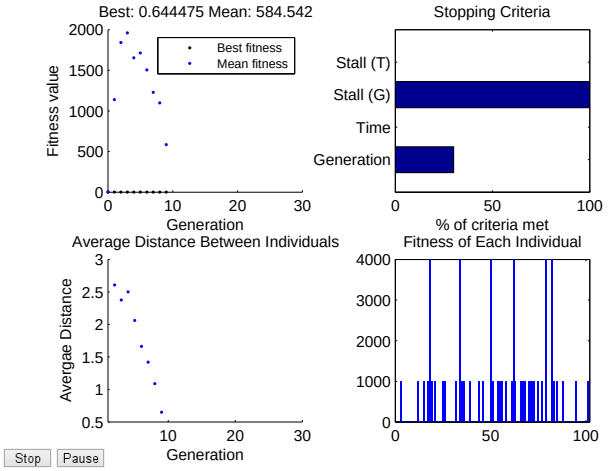

(c) Four sensors

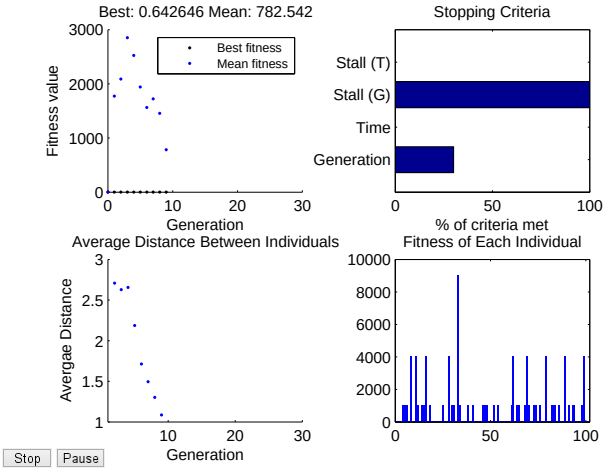

(d) Five sensors

Figure 6: Genetic Algorithms optimisation evolution in Hanoi DMA

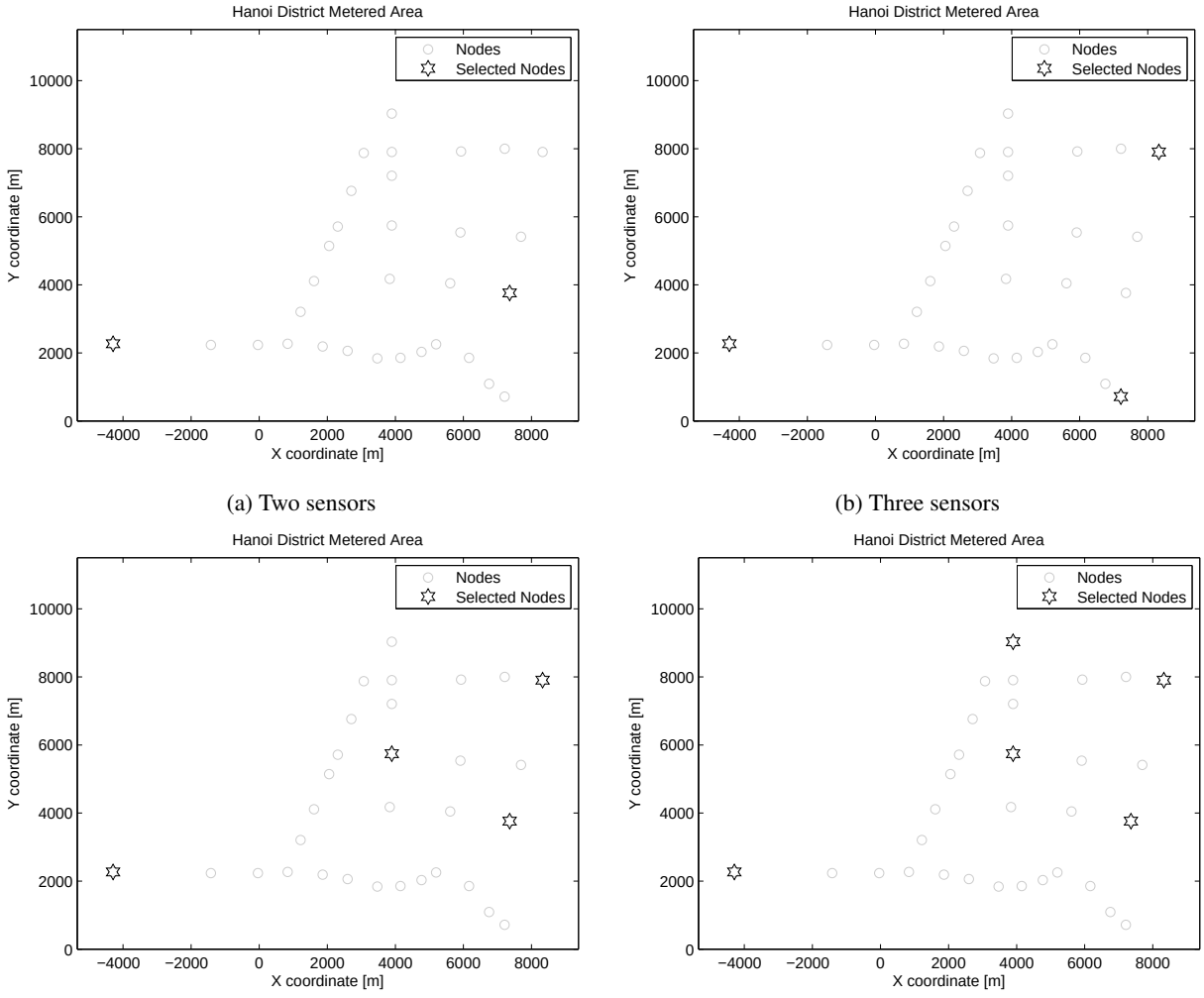

(a) Two sensors

(b) Three sensors

(c) Four sensors

(d) Five sensors

Figure 7: Sensor placement in Hanoi DMA

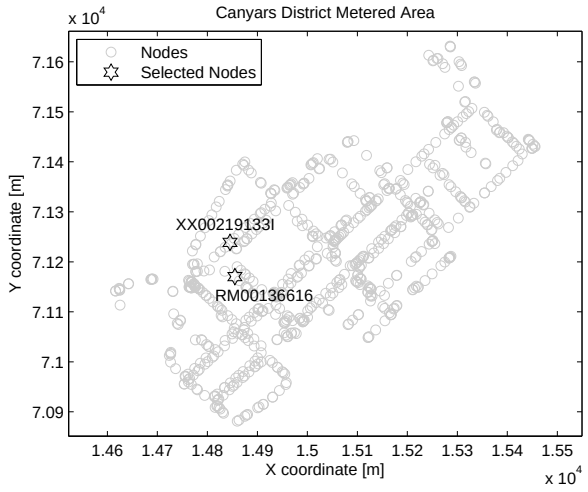

(a) Two sensors

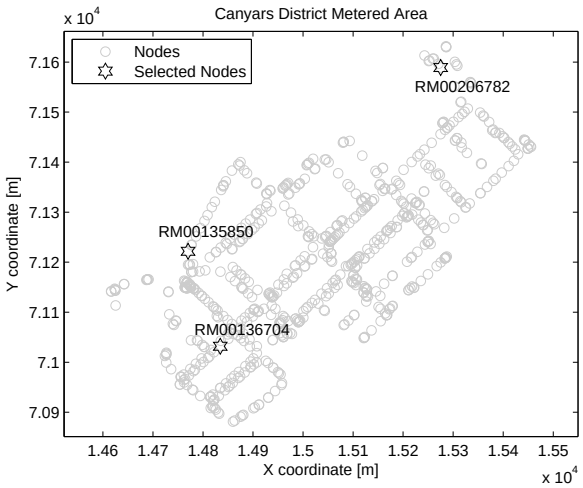

(b) Three sensors

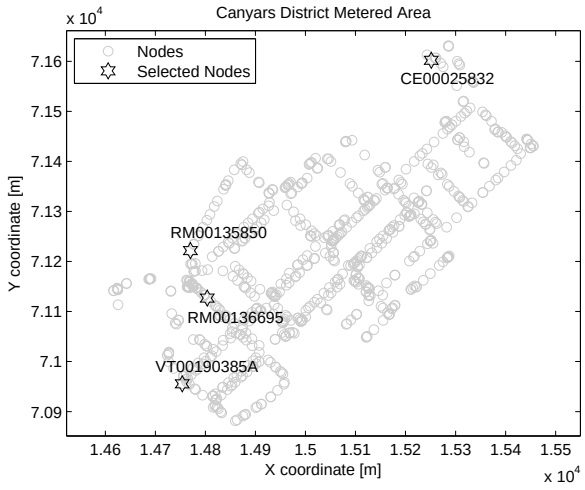

(c) Four sensors

Figure 8: Sensor placement in Canyars DMA

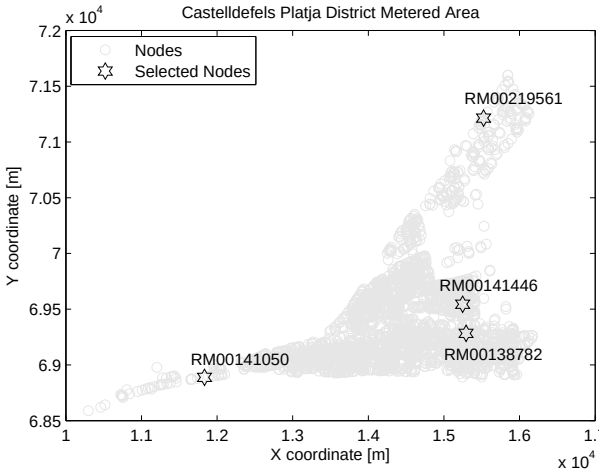

(a) Four sensors

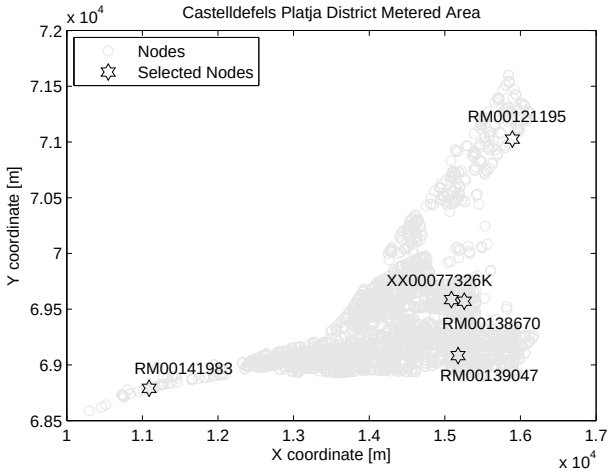

(b) Five sensors

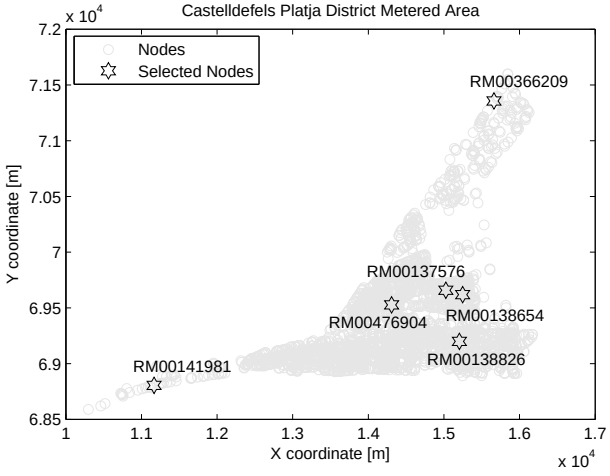

(c) Six sensors

Figure 9: Sensor placement in Castelldefels Platja DMA